

Turn-Off-and-On: Chemosensing Ensembles for Sensing Chloride in Water by Fluorescence Spectroscopy

Thomas Riis-Johannessen, Kurt Schenk, and Kay Severin*

Institut des Sciences et Ingénierie Chimiques, Institut de Physique des Systèmes Biologiques, Ecole Polytechnique Fédérale de Lausanne (EPFL), 1015 Lausanne, Switzerland

Received June 28, 2010

The recognition and sensing of aqueous chloride by synthetic receptors is a challenging task. Herein we apply the chemosensing ensemble methodology to optically detect chloride in water at near physiological pH. Variants based on two closely related receptors have been explored. The sensors can be obtained in situ by mixing a rhodium complex, a bidentate *N,N*-chelate ligand, and a fluorescent dye in buffered aqueous solution. Upon mixing the sensor components, the rhodium complex binds to the *N,N*-chelate ligand to yield a metal-based receptor. This latter associates with the fluorophore to give a non-emissive ground-state complex. The chemosensing ensembles respond to chloride via a turn-on fluorescence signal and can be used for optical detection of chloride down to mid-micromolar concentrations.

Introduction

Optical chloride sensors can generally be classified into one of two groups. One approach relies on non-specific transient interactions between an excited-state fluorophore and chloride, which results in quenching of the emission of the fluorophore (i.e., dynamic quenching).¹ This method is ideally suited for detection in the millimolar range, but lacks in sensitivity for more dilute samples of less than 1 mM chloride content.¹ Alternatively, chloride detection can be achieved by covalently linking a receptor with a chromo- or fluorophore, to yield a *conjugate* chemosensor.^{2,3} Binding of Cl[−] to the receptor causes a pronounced change in the optical properties of the molecule, which can be monitored using a suitable spectroscopic technique. The conjugate approach has the advantage that the binding site and chromo- or fluorophore can be tuned to yield optimal signal output, sensitivity, and selectivity. On the other hand, it often involves extensive synthetic effort and, because of solubility restrictions, can be limited to sensing in organic media or aqueous/organic mixtures. Furthermore, despite a growing appreciation for the use of Lewis-acidic metal centers as binding

sites for receptors,⁴ the majority of such sensors rely on electrostatics and/or hydrogen bonding to bind the anion, interactions which are largely diminished in competitive polar and/or protic solvents.⁵ They can therefore lack in sensitivity when substantial amounts of water are present.^{2d}

Recently, we described preliminary attempts to address some of these issues.⁶ Our work was inspired by reports from the context of medicinal chemistry that half-sandwich complexes of the type $[(\eta^6\text{-arene})\text{Ru}(\text{en})(\text{H}_2\text{O})]^{2+}$ (en = ethylenediamine) can coordinate Cl[−] in water with log *K* values of up to 2.1.⁷ Accordingly, we constructed a chemosensing ensemble by combining complex $[(\text{Cp}^*\text{Rh})_2(\mu\text{-OH})_3](\text{NO}_3)$ with the chelate ligand Ferrozine (Fz) and fluorophore 8-hydroxypyrene-1,3,6-trisulfonate in the presence of the cationic surfactant cetyltrimethylammonium hydrogensulfate (Scheme 1). The chelate ligand reacts with the Rh complex to give the monomeric aqua complex $[\text{Cp}^*\text{Rh}(\text{Fz})(\text{H}_2\text{O})]$ (**1**). This complex acts as a receptor for chloride. The adduct **1**·Cl[−] partitions in the micelles formed by the surfactant and quenches the fluorescence of the dye, which is likewise bound to the micelles. As a result, one observes a pronounced turn-off fluorimetric response. Preferential solvation of **1**·Cl[−] within the micelle also causes an apparent increase of the affinity of receptor **1** for Cl[−], thereby enhancing the detection limits of the sensor and allowing for the quantitative detection of chloride in water down to low micromolar concentrations.⁶

*To whom correspondence should be addressed. E-mail: kay.severin@epfl.ch.

(1) (a) Geddes, G. D. *Meas. Sci. Technol.* **2001**, *12*, R53–R88. (b) Jayaraman, S.; Verkman, A. S. *Biophys. Chem.* **2000**, *85*, 49–57.

(2) (a) Gale, P. A. *Chem. Commun.* **2011** DOI: 10.1039/c0cc00656d. (b) Gale, P. A. *Chem. Commun.* **2008**, 4525–4540. (c) Gunnlaugsson, T.; Glynn, M.; Tocchi, G. M.; Kruger, P. E.; Pfeffer, F. M. *Coord. Chem. Rev.* **2006**, *250*, 3094–3117. (d) Kubik, S.; Reyheller, C.; Stüwe, S. J. *Inclusion Phenom. Macrocyclic Chem.* **2005**, *52*, 137. (e) Suksai, C.; Tuntulani, T. *Chem. Soc. Rev.* **2003**, *32*, 192–202. (f) Martínez-Mañez, R.; Sancenón, F. *Chem. Rev.* **2003**, *103*, 4419–4476. (g) Beer, P. D.; Gale, P. A. *Angew. Chem., Int. Ed.* **2001**, *40*, 486–516.

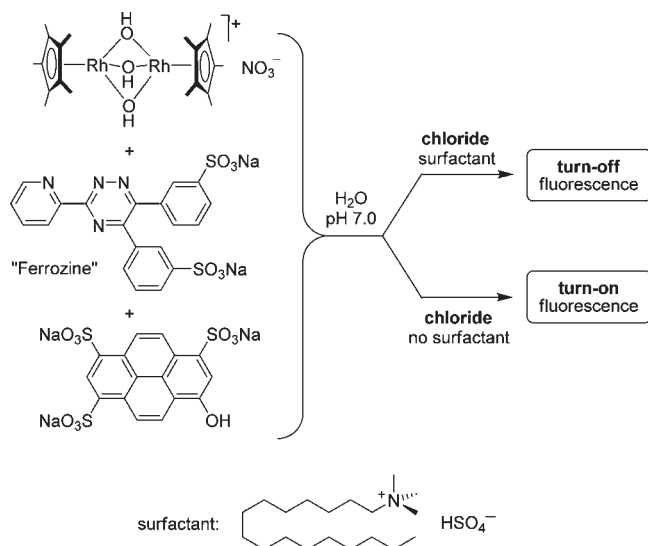
(3) (a) Spichigger-Keller, U. E. *Chemical sensors and biosensors for medical and biological applications*; Wiley: New York, 2007. (b) Mancin, F.; Rampazzo, E.; Tecilla, P.; Tonellato, U. *Chem.—Eur. J.* **2006**, *12*, 1844–1854.

(4) (a) Steed, J. W. *Chem. Soc. Rev.* **2009**, *38*, 506–519. (b) Beer, P. D.; Hayes, E. H. *Coord. Chem. Rev.* **2003**, *240*, 167–189.

(5) Steed, J. W.; Atwood, J. L. *Supramolecular Chemistry*; Wiley: New York, 2009.

(6) Riis-Johannessen, T.; Severin, K. *Chem.—Eur. J.* **2010**, *16*, 8291–8295.

(7) Wang, F.; Chen, H.; Parsons, S.; Oswald, I. D. H.; Davidson, J. E.; Sadler, P. J. *Chem.—Eur. J.* **2003**, *9*, 5810–5820.

Scheme 1. Chemosensing Ensembles for the Fluorimetric Detection of Chloride^a

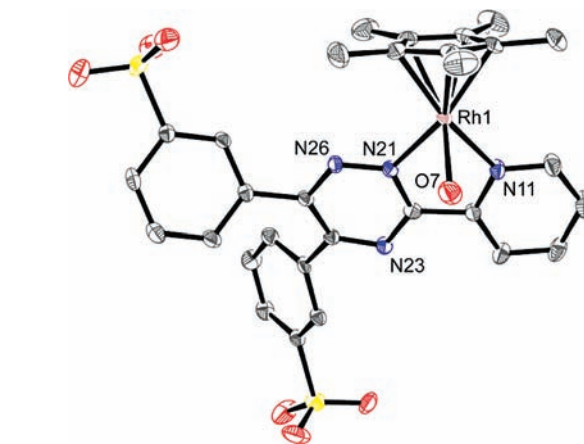
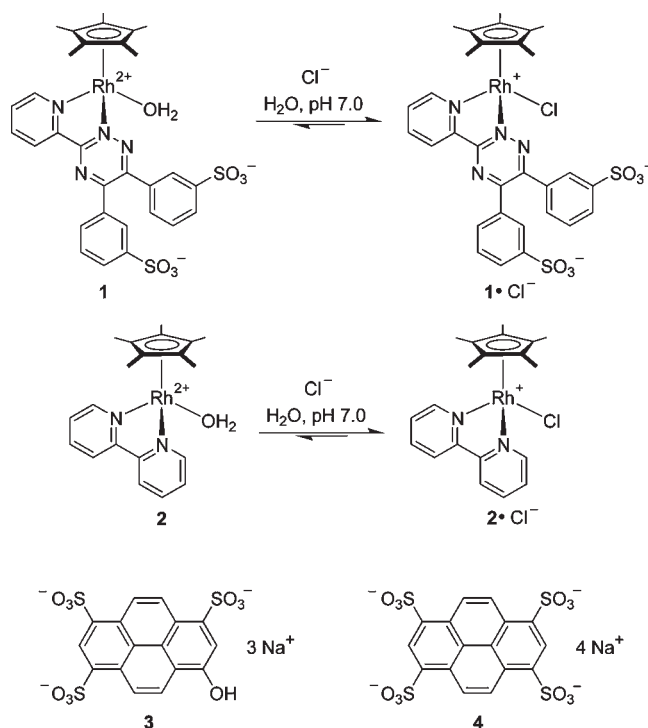
One drawback of this approach is that it relies on surfactants to function, which can limit potential applications.⁸ We therefore decided to explore how the various components interact *in the absence* of surfactant micelles. Remarkably, it was found that the system is switched from a turn-off fluorescence sensor to a turn-on sensor when the surfactant is omitted (Scheme 1). Furthermore, it was observed that the selectivity and the sensitivity of the chemosensing ensemble can be modulated by variation of the chelate ligand. Structural and spectroscopic studies about these sensors are described below.

Results and Discussion

Synthesis and Characterization of Receptors **1** and **2**.

Air-stable and water-soluble receptors **1** and **2** (Scheme 2) can be prepared *in situ* by combining the hydroxy-bridged rhodium(III) dimer [(Cp* Rh)₂(μ -OH)₃](NO₃) with 2 equiv of commercially available Ferrozine or 2,2'-bipyridine, respectively, in MOPS buffer solution (50 mM, pH 7.0; MOPS = 3-(*N*-morpholino)propanesulfonic acid).⁶ Acidity constants for monodeprotonation of the weakly bound aqua ligands in **1** and **2** are both $\text{p}K_{\text{a}} \approx 8.3$.^{6,9} At neutral pH, therefore, the receptors exist in water as their neutral zwitterionic (**1**) and dicationic (**2**) aqua complexes.

While both aqua- and chloro-adducts of **2** have already been crystallographically characterized,^{9,10} no structural investigations into Ferrozine, or indeed any of its metal complexes, have appeared in the literature despite its now widespread use as co-reagent for the spectrophotometric

**Figure 1.** Ortep plot of **1** with thermal ellipsoids shown at 30% probability level. Hydrogens and co-crystallized water molecules are omitted for clarity. Selected bond lengths: Rh–Cp* 2.139(5)–2.168(4) Å; Rh–O7 2.177(4) Å; Rh–N11 2.132(4) Å; Rh–N23 2.079(3) Å.**Scheme 2.** Chloride Receptors **1** and **2** and the Fluorescent Dyes **3** and **4**

determination of iron(II).¹¹ We therefore grew crystals of **1** from pH neutral water by slow evaporation and determined its structure by X-ray diffraction analysis. The solid-state structure is shown in Figure 1. The complex is charge neutral and adopts a piano-stool geometry, typical of (arene)M-aqua/chloro complexes (M = Rh^{III}, Ru^{II}) wherein two of the coordination sites opposite the π -ligand are bound by a neutral *N,N*-chelate ligand.^{7,9,10} The bond lengths and angles are largely unremarkable. Worth noting, however, is the connectivity of the Fz ligand: the two sulfonate groups are located in the *meta*-positions of the phenyl rings (see Scheme 1) and *not* the

(8) Our approach would not be applicable in membrane transport assays. See for example: (a) Senagish, J. L.; Davies, A. P. *Chem. Commun.* **2005**, 5781–5783. (b) Izzo, I.; Licen, S.; Maulucci, N.; Autore, G.; Marzocco, S.; Tecilla, P.; de Riccardis, F. *Chem. Commun.* **2008**, 2986–2988.

(9) Daddi, L.; Elias, H.; Frey, U.; Hörnig, A.; Koelle, U.; Merbach, A. E.; Paulus, H.; Schneider, J. S. *Inorg. Chem.* **1995**, *34*, 306–315.

(10) Ogo, S.; Hayashi, H.; Uehara, K.; Fukuzumi, S. *Appl. Organomet. Chem.* **2005**, *19*, 639–643.

(11) (a) Stookey, L. L. *Anal. Chem.* **1970**, *42*, 779–781. (b) Carter, P. *Anal. Biochem.* **1971**, *40*, 450–458. (c) Gibbs, C. R. *Anal. Biochem.* **1971**, *48*, 1197–1201.

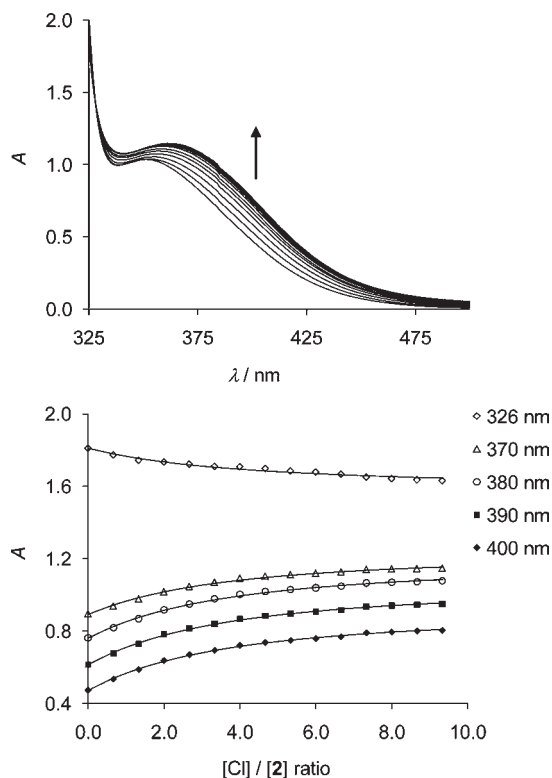


Figure 2. Top: changes in UV-vis spectra observed upon titration of NaCl (0–5 mM) into a solution of **2** (500 μM) in MOPS buffer solution (50 mM, pH 7.0). Bottom: absorbance as a function of [Cl⁻]/[**2**] ratio for five selected wavelengths. The lines were obtained by fitting the data to a 1:1 binding isotherm.

para-positions, as originally proposed on the basis of IR stretching frequencies^{11a} and subsequently featured in numerous publications.^{11,12} This substitution pattern has been confirmed by ¹H NMR spectroscopy, which shows triplet and singlet multiplicities for the protons of the two phenylsulfonate groups,⁶ as opposed to the simple doublets that would be expected for *para*-substitution.

Chloride Binding and Signal Transduction. The addition of NaCl to MOPS buffer solutions (50 mM, pH 7.0) of **1** or **2** causes smooth but subtle variations in absorbance (300 ≤ λ ≤ 600 nm) which can be fitted to 1:1 binding isotherms, giving log $K_{1 \cdot Cl^-} = 2.82(5)$ and log $K_{2 \cdot Cl^-} = 2.80(5)$ (Figure 2). For solutions of [**1**]_{tot} = [**2**]_{tot} = 500 μM, the aqua ligands are ~95% displaced by Cl⁻ when [NaCl]_{tot} = 20.0 mM. The association constants are comparable to those reported for much more elaborate receptors which bind Cl⁻ via multiple hydrogen bonds,² despite the former relying on the formation of only *one* metal–ligand coordinative interaction. Their implications for chloride sensing in water are thus very promising. However, the absorption spectra of **1**·Cl⁻ or **2**·Cl⁻ are not sufficiently distinct from their aqua precursors for a direct colorimetric read-out.

To signal the binding event we introduced 8-hydroxy-1,3,6-pyrenetrisulfonate (**3**), a commercially available and

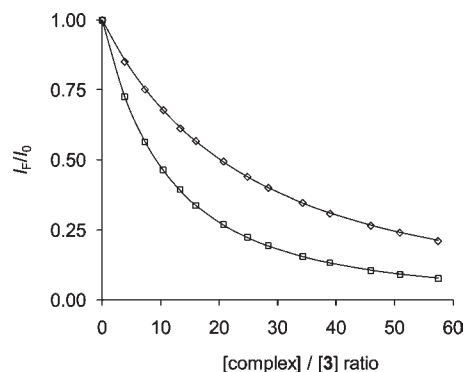


Figure 3. Relative emission intensity at 510 nm (λ_{ex} = 480 nm) of a MOPS buffer solution (50 mM, pH 7.0) containing **3** (12.5 μM) and variable amounts (0–700 μM) of **1** (◇) and **2** (□). The lines were obtained by fitting the data to the equilibrium models described in the main text.

water-soluble fluorescent dye which emits light at 510 nm with high quantum yield.^{13,14} As demonstrated in our previous work, emission from **3** is efficiently quenched by chloro-receptor complex **1**·Cl⁻, but *only* when the two are co-confined within the nanosized volume of a surfactant micelle.⁶ Quenching was tentatively attributed to electron transfer from the excited-state fluorophore to **1**·Cl⁻. However, micellized **3** is largely unaffected by the naked receptor **1** since the latter preferentially resides in the bulk aqueous phase.

Without surfactant, **1** and **3** can no longer phase-separate, and a different situation may be envisaged: the two associate via supramolecular interactions, leading to a non-emissive ground-state complex.¹⁴ Chloride could then be signaled by one of two mechanisms: (1) If the fluorophore binds directly or nearby to the rhodium(III) center, addition of Cl⁻ would result in its displacement, causing an increase in fluorescence emission.^{14a–c} Sensors of this kind are generally termed indicator displacement assays (IDAs),^{3,15} and they have been successfully applied for sensing various anions¹⁶ but not, to the best of our knowledge, for chloride. (2) Alternatively, the complex could act as a ditopic receptor to which both **3** and Cl⁻ bind concomitantly.^{14d} Provided the two sites are either mechanically or electronically coupled, chloride recognition would then modulate the optical properties of **3** in an analogous way to a classical conjugate chemosensor.

The binding of receptors **1** and **2** to fluorophore **3** was first investigated by steady-state fluorescence spectroscopy. As can be seen in Figure 3, the emission at λ_{em} = 510 nm of a MOPS buffer solution (50 mM, pH 7.0) containing **3** (12.5 μM) is dramatically attenuated upon addition of **1** or **2**. The effect is

(13) de Borja, E. B.; Amaral, C. L. C.; Politi, M. J.; Villalobos, R.; Baptista, M. S. *Langmuir* **2000**, *16*, 5900–5907.

(14) For examples of **3** used in chemosensing ensembles see: (a) Gamsey, S.; Miller, A.; Olmstead, M. M.; Beavers, C. M.; Hirayama, L. C.; Pradhan, S.; Wessling, R. A.; Singaram, B. *J. Am. Chem. Soc.* **2007**, *129*, 1278–1286. (b) Cordes, D. B.; Gamsey, S.; Sharrett, Z.; Miller, A.; Thoniyot, P.; Wessling, R. A.; Singaram, B. *Langmuir* **2005**, *21*, 6540–6547. (c) Neelakandan, P. P.; Hariharan, M.; Ramaiah, D. *J. Am. Chem. Soc.* **2006**, *128*, 11334–11335. (d) Gao, J.; Rochat, S.; Qian, X.; Severin, K. *Chem.—Eur. J.* **2010**, *16*, 5030–5070.

(15) Nguyen, B. T.; Anslyn, E. V. *Coord. Chem. Rev.* **2006**, *250*, 3118–3127.

(16) See for example: (a) Han, M. S.; Kim, D. H. *Angew. Chem., Int. Ed.* **2002**, *41*, 3809–3811. (b) Fabbrizzi, L.; Marcotte, N.; Stomeo, F.; Taglietti, A. *Angew. Chem., Int. Ed.* **2002**, *41*, 3811–3814. (c) Boiocchi, M.; Bonizzoni, M.; Fabbrizzi, L.; Piovani, G.; Taglietti, A. *Angew. Chem., Int. Ed.* **2004**, *43*, 3847–3852. (d) Fabbrizzi, L.; Leone, A.; Taglietti, A. *Angew. Chem., Int. Ed.* **2001**, *40*, 3066–3069.

(12) For selected examples see: (a) Uma, R.; Palaniandavar, M.; Butcher, R. J. *J. Chem. Soc., Dalton Trans.* **1996**, 2061–2066. (b) Akl, M. A.; Mori, Y.; Sawada, K. *Anal. Sci.* **2006**, *22*, 1169–1174. (c) Körner, M.; Tregloan, P. A.; van Eldik, R. *Dalton Trans.* **2003**, 2710–2717. (d) Guo, M.; Perez, C.; Wei, Y.; Rapoza, E.; Su, G.; Bou-Abdallah, F.; Chasteen, M. D. *Dalton Trans.* **2007**, 4951–4961. (e) Thompsen, J. C.; Mottola, H. A. *Anal. Chem.* **1984**, *56*, 755–757.

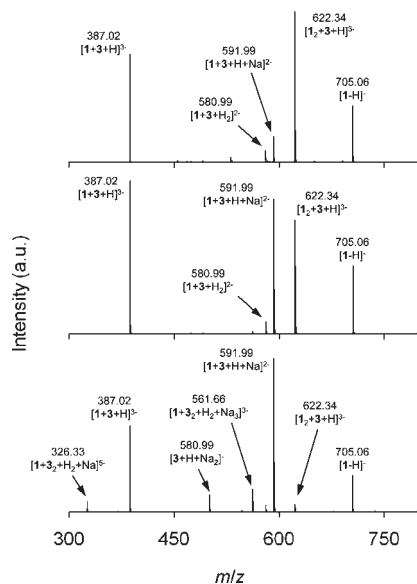


Figure 4. Negative scan ESI mass spectra of aqueous solutions (pH 7.0) containing **1** and 0.5 (top), 1.0 (middle), and 5.0 (bottom) equiv of **3**. The selected assignments are made on the basis that (1) **3** is in its fully ionized, tetra-anionic form, and (2) **2** is missing its aqua ligand.

clearly more pronounced for dicationic receptor **2**, which reduces the fluorescence emission intensity I_F to $< 10\%$ of its initial value I_0 at a concentration of $[2]_{\text{tot}} = 700 \mu\text{M}$ (cf. $I_F/I_0 \approx 25\%$ for $[1]_{\text{tot}} = 700 \mu\text{M}$). Nonetheless, both data sets can be satisfactorily fitted to the same equilibrium model, which considers the successive fixation of two receptors to one fluorophore to give two non-emissive complexes. This gives best-fit parameters of $\log K_1 = 3.53(5)$ and $\log K_2 = 2.86(4)$ for **1** and $\log K_1 = 3.89(5)$ and $\log K_2 = 3.20(5)$ for **2**. Consistently higher values for **2** likely reflect the stronger electrostatic attraction occurring between the oppositely charged receptor and fluorophore components.

The implied ground-state complexes between **1** and **3** were evidenced by electrospray-ionization mass spectrometry (ESI-MS). In negative scan mode, the mass spectra of solutions containing **1** (100 μM) and increasing amounts of **3** ($0 \leq [3]_{\text{tot}} \leq 2.0 \text{ mM}$) show peaks corresponding to various 1:1 and 1:2 adducts (Figure 4), consistent with the equilibrium model proposed from the emission data. The 1:2 adducts dominate for $[3]/[1]$ ratios of ≤ 1 , while 1:1 adducts and related fragments become more abundant for $[3]/[1] \geq 1$. With an appreciable excess of **3**, however, peaks for polyanionic 2:1 adducts also start to appear, suggesting that larger aggregates can form in solution.

Various binding modes can be envisaged for the association between the receptors **1** and **2** and fluorophore **3**: (1) **3** could coordinate directly to the rhodium(III) centers via its hydroxyl function which, with a ground-state pK_a of 7.4,¹³ is already partly ionized at pH 7.0. (2) Alternatively, the aromatic ring system of the fluorophore could interact with the Cp* ligands via electrostatic attraction, dispersive $\pi \cdots \pi/\text{CH} \cdots \pi$ interactions, and/or hydrophobic effects, in a manner similar to that proposed for cationic benzyl-substituted viologens^{14a-c} and an (arene)-Ru^{II}-based metallamacrocycle.^{14d}

To further probe the receptor-fluorophore interactions in the millimolar concentration range we performed

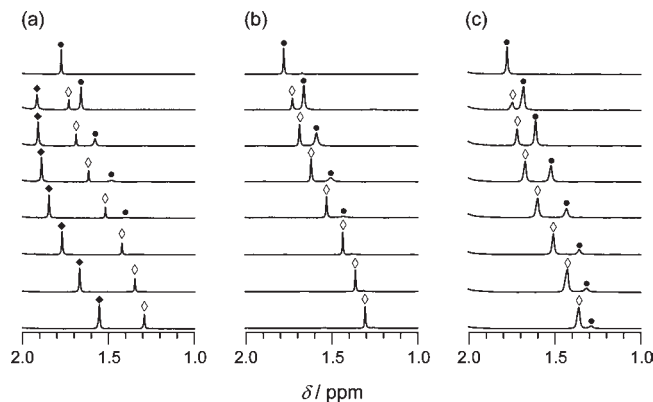


Figure 5. Cp* resonances in the ^1H NMR spectra of solutions (v/v $\text{H}_2\text{O}/\text{D}_2\text{O}$ 95:5) containing **1** (1.0 mM) and variable amounts of **3** at (a) pH 7.0 and (b) pH 5.5, and (c) **4** at pH 7.0. The total concentrations of **3/4** are (from top to bottom): 0, 1.0, 1.9, 3.7, 6.9, 12.1, 19.5, 30.8 mM.

^1H NMR investigations. The Cp* resonances for a series of spectra obtained on titrating **3** into a MOPS buffer solution (50 mM, pH 7.0) of $[1]_{\text{tot}} = 1.0 \text{ mM}$ are shown in Figure 5a. As can be seen, the system displays an unexpectedly high level of complexity under these conditions. When **3** is added, the singlet for the Cp* ligand of **1** first splits into three, one initial (\bullet) and two new (\blacklozenge and \diamond), peaks. On further addition, the two new peaks then grow at the expense of the initial one, while all three are gradually shifted to lower frequency, invoking the onset of second-order interactions whose exchange kinetics are fast on the NMR time scale. Taken together, this implies that a complex equilibrium involving at least six species (including free **1**) is established upon addition of **3**.

Although the structures of these species are not clear from the above data, performing the titration with MES buffer (50 mM; MES = 2-(*N*-morpholino)ethanesulfonic acid) at pH 5.5 yields some useful information about the nature of the interactions at play. As can be seen in Figure 5b, the initial singlet now splits into only two signals (\diamond and \bullet) on addition of **3**, both of which then undergo similar shift changes with increasing $[3]_{\text{tot}}$ to those observed at pH 7.0. The most downfield peak from Figure 5a (\blacklozenge) does not appear; otherwise, the two series of spectra are essentially superimposable.

Since the hydroxyl group on **3** is fully protonated at pH 5.5, it stands to reason that the more intense, downfield signal (\blacklozenge) only observed at pH 7.0 is due to a hydroxyl-bound species (cf. the first of the two scenarios described above). The possibility that the two new peaks (\blacklozenge and \diamond) simply correspond to acidic and basic forms of the same complex can be discounted on the basis that hydroxyl proton exchange is typically too fast on the ^1H NMR time scale for separate signals to be observed. We therefore suspect that the more upfield of the two new peaks (\diamond) is due to a sulfonate-bound species. Indeed, this is supported by Figure 5c which shows how the Cp* protons evolve on adding the all-sulfonate analogue of **3**, pyrene-1,3,6,8-tetrasulfonate (**4**): Once again the initial singlet collapses into two new peaks, the chemical shifts of which then evolve in a remarkably similar fashion to those in Figure 5a. We note, however, that adding up to 30 equiv of Na_2SO_4 has no discernible effect on the spectra. Accordingly, if the species which gives rise the second

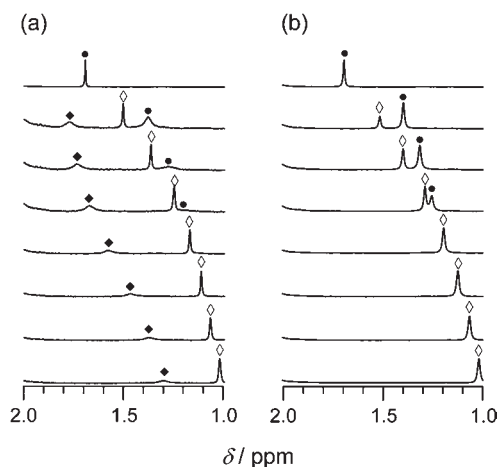


Figure 6. Cp* resonances in the ^1H NMR spectra of solutions (v/v $\text{H}_2\text{O}/\text{D}_2\text{O}$ 95:5) containing **2** (1.0 mM) and variable amounts of (a) **3** and (b) **4** at pH 7.0. The total pyrene concentrations are (from top to bottom): 0, 1.0, 1.9, 3.7, 6.9, 12.1, 19.5, 30.8 mM.

peak (\diamond) does feature a $\text{Rh}^{\text{III}}-\text{O}_3\text{S}$ interaction, it is likely supplemented by additional attractive interactions (e.g., electrostatic and/or dispersive $\pi\cdots\pi/\text{CH}\cdots\pi$ interactions).

The Cp* peaks are all systematically shifted to lower frequency upon addition of **3** (or **4**). We interpret this as evidence that a third, more labile binding mode exists, and we suspect that the aromatic regions of the fluorophore and the Cp*Rh unit (case 2, vide supra). That the two new peaks (\blacklozenge and \diamond) also experience upfield shifts furthermore suggests that more than one fluorophore can concomitantly bind to the receptor, giving putative $1\cdot 3_2$ complexes. This is consistent with the gas-phase ESI-MS studies, which also indicated the presence of such species in solutions with **3/1** ratios of $\gg 1$.

The dicationic receptor **2** displays similar multiphasic behavior upon addition of **3** or **4** (Figure 6). At pH 7.0 two new peaks appear (\blacklozenge and \diamond) and grow at the expense of the initial one (\bullet), though the species which gives rise to the more upfield of these (\diamond) is now formed preferentially (cf. Figure 5).

To gain further insight into these systems, we attempted to grow single crystals for X-ray diffraction studies. For complexes of **3** with **1** or **2** this proved largely unsuccessful, probably owing to the large number of species present in any given mixture of the various components. We did, however, obtain co-crystals of **4** and **2** by slowly evaporating an aqueous solution (pH 7.0) containing the two components in a 1:2 ratio, respectively. The crystal structure was solved in $P\bar{1}$ ($Z = 1$), and it features charge-neutral aggregates composed of two dicationic complexes **2** and one tetra-anionic fluorophore **4**. In the solid-state, **4** straddles an inversion center, while the two crystallographically equivalent half-sandwich complexes **2** lie above and below it, both with their Cp* ligands oriented toward the central pyrene ring system. The five-membered Cp* rings are essentially coplanar with the 16 carbon atoms of **4** (dihedral angle: $3(1)^\circ$), and the planes are separated by centroid-centroid distances of 3.6(1) Å, typical for $\pi-\pi$ stacking interactions. Interestingly, complexes **2** both retain their aqua ligands and so direct coordination of **4** to the rhodium(III) centers does not occur in this case.

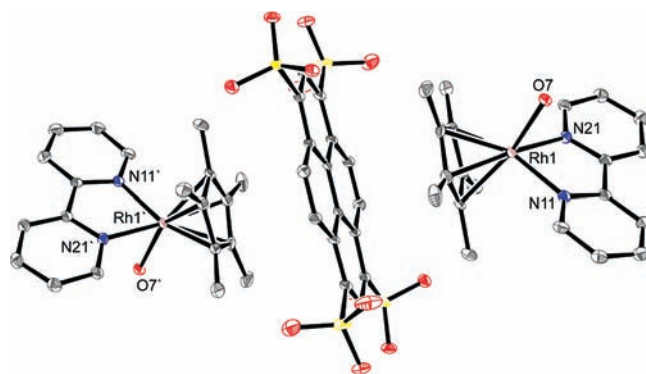


Figure 7. Ortep plot of **2**·**4** with thermal ellipsoids shown at 30% probability level. Hydrogens and interstitial waters are omitted for clarity. Selected bond lengths: Rh–Cp* 2.136(4)–2.169(4) Å; Rh–O7 2.149(2) Å; Rh–N11 2.105(3); Rh–N21 2.108(3) Å.

There are, however, specific $\text{O}-\text{H}\cdots\text{O}(\text{SO}_2\text{R})$ and $\text{C}-\text{H}\cdots\text{O}(\text{SO}_2\text{R})$ hydrogen-bonds between protons on the aqua and bipy ligands in **2** and the sulfonate groups from adjacent pyrene-1,3,6,8-tetrasulfonate moieties. Similar interactions also link the ion pairs to a well-defined network of interstitial water molecules (seven per asymmetric unit).

The dispersive $\pi\cdots\pi$ interactions between **4** and **2** are reminiscent of those previously observed in co-crystals of **3** with several cationic viologen derivatives.^{14a,17} The latter were unambiguously shown to persist in aqueous solution, although factors such as electrostatic attraction and hydrophobic effects almost certainly contributed. We propose that this interaction likewise exists in solutions containing **3** and receptors **1** or **2**, and that it accounts for at least one of the binding modes observed by ^1H NMR. Indeed, given the close proximity and orientation of the Cp* protons with respect to the shielding ring currents of **4** (Figure 7), it most likely manifests itself as the upfield shifts which are systematically observed for all Cp* peaks of **1** or **2** upon addition of **3**. That such interactions are likely fast on the NMR time scale is also consistent with the fact that complexation is evidenced by changes in chemical shift, and not by the appearance of new peaks.

Fluorescence Chloride Assay. Having established that both receptors form non-emissive ground-state complexes with **3**, we investigated whether they could be used as chemosensing ensembles for the detection of chloride. In principle, chloride could be signaled by any combination of the two transduction mechanisms discussed earlier (vide supra) since **3** appears to interact with the receptors via at least three different binding modes, one of which does not involve coordination to the chloride recognition site on the rhodium(III) center (see Figure 7).

First, a sensing ensemble composed of **1** (500 μM) and **3** (50 μM) in MOPS buffer solution (100 mM, pH 7.0) was prepared. Under these conditions excitation at $\lambda_{\text{ex}} = 480$ nm gives rise to only weak fluorescence emission since about 70% of the fluorescent dye is in its non-emissive complexed form (as estimated from the successive formation constants discussed earlier). Addition of Cl^- (30.0 mM) then restores the original fluorescence, amounting to an increase of about 325% in emission intensity at

(17) Wang, C.; Guo, Y.; Wang, Y.; Xu, H.; Wang, R.; Zhang, X. *Angew. Chem., Int. Ed.* **2009**, *48*, 8962–8965.

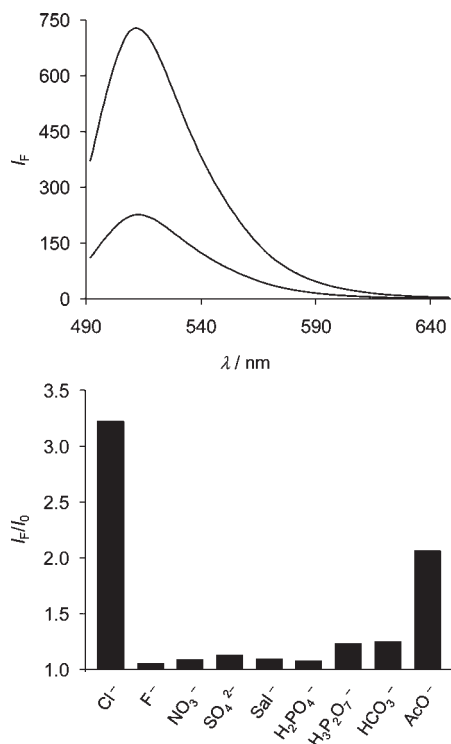


Figure 8. Top: fluorescence emission spectra of sensing ensemble composed of complex **1** (500 μM) and **3** (50 μM) in the absence and in the presence of NaCl (30.0 mM). Bottom: relative fluorescence emission at 510 nm ($\lambda_{\text{ex}} = 480$ nm) in the presence of NaCl, NaF, NaNO₃, Na₂SO₄, NaSal (Sal = salicylate), NaH₂PO₄, Na₄P₂O₇, NaHCO₃, NaOAc, NaHCO₃, NaNO₃ (30.0 mM each). The spectra were recorded in aqueous MOPS buffer solution (100 mM, pH 7.0).

$\lambda_{\text{em}} = 510$ nm (Figure 8). The response is quite selective for chloride over other relevant anions. In particular, phosphate and pyrophosphate, both known to coordinate Cp*Rh^{III} centers,¹⁸ elicit only minor responses. The sensor does succumb to the usual interference problems with the heavier halides (Br^- and I^-) and pseudohalide CN^- , presumably because of their superior affinity for direct coordination of the rhodium(III) center in **1** and related complexes.⁹ Such limitations are, however, of little importance given the low concentrations at which these anions typically occur in nature. Acetate also provokes a turn-on signal of about 50% of that observed for Cl^- .

We have also measured the fluorescence of samples containing variable NaCl concentrations of 0–30 mM. The relative emission versus $[\text{Cl}]_{\text{tot}}$ profile is shown in Figure 9. The resulting data can be used as a calibration curve for the sensing of Cl^- with a dynamic range of approximately 0.1–30 mM and with lower and upper limits of quantification of about 300 μM and 20 mM, respectively. For comparison, the signals observed for Cl^- (0–10 mM) in the presence of NaF, NaNO₃, Na₂SO₄, NaSal (Sal = salicylate), NaH₂PO₄, Na₄P₂O₇, NaHCO₃, NaOAc, NaHCO₃, NaNO₃ (1.0 mM each) are also shown. For concentrations of $[\text{Cl}]_{\text{tot}} < 10$ mM, the two curves are more or less superimposable. The sensor thus appears to function well in the presence of small quantities of potentially interfering electrolytes.

(18) (a) Smith, D. P.; Kohen, E.; Maestre, M. F.; Fish, R. H. *Inorg. Chem.* **1993**, *32*, 4119–4122. (b) Buryak, A.; Pozdnoukhov, A.; Severin, K. *Chem. Commun.* **2007**, 2366–2368. (c) Buryak, A.; Zaubitzer, F.; Pozdnoukhov, A.; Severin, K. *J. Am. Chem. Soc.* **2008**, *130*, 11260–11261.

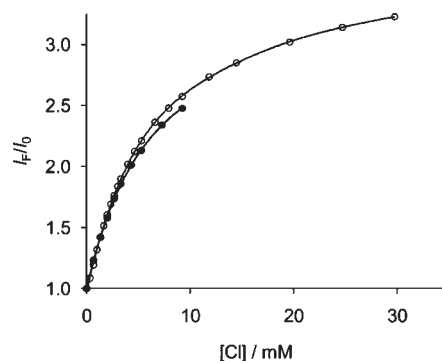


Figure 9. Relative fluorescence emission at 510 nm ($\lambda_{\text{ex}} = 480$ nm) of the sensing ensemble composed of complex **1** (500 μM) and **3** (50 μM) upon addition of NaCl with (●) and without (○) all other anions present at 1.0 mM. The spectra were recorded in aqueous MOPS buffer solution (100 mM, pH 7.0).

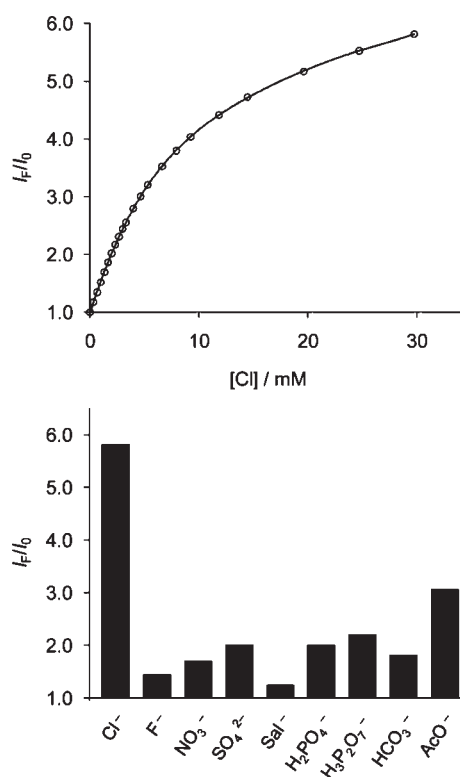


Figure 10. Relative fluorescence emission at 510 nm ($\lambda_{\text{ex}} = 480$ nm) of the sensing ensemble composed of complex **2** (500 μM) and **3** (50 μM) in the presence of (top) variable amounts of NaCl and (bottom) NaCl, NaF, NaNO₃, Na₂SO₄, NaSal (Sal = salicylate), NaH₂PO₄, Na₄P₂O₇, NaHCO₃, NaOAc, NaHCO₃, NaNO₃ (30.0 mM each). The spectra were recorded in aqueous MOPS buffer solution (100 mM, pH 7.0).

Finally, we examined the impact of exchanging neutral zwitterionic receptor **1** for dicationic receptor **2**. Adding chloride to a chemosensing ensemble based on **2** elicits a similar turn-on response, except that the fluorescence intensity now increases by about 600% (cf. 325% for the sensor based on **1**). This is due to the fact that 85% of $[\text{3}]_{\text{tot}}$ is initially in its complexed form prior to introducing the analyte. Accordingly, the dynamic range is larger under these conditions; it spans approximately 0.05–30 mM in concentration (Figure 10). Likewise, the lower and upper limits of quantification can be estimated at about 150 μM and 30 mM, respectively. This improvement in sensitivity

does, however, come at the expense of poorer selectivity. The chemosensing ensemble with **2** responds to other anions via emission intensity amplifications ranging from 50%, for salicylate, to 300%, for acetate. In particular, the signals generated by anions such as NO_3^- , SO_4^- , H_2PO_4^- , $\text{H}_3\text{P}_2\text{O}_7^-$, and HCO_3^- amount to 15–30% of the total increase observed on adding 30.0 mM NaCl. The sensor response observed in the presence of all other anions (1.0 mM) is also severely dampened with respect to that observed for pure chloride. The use of **2** in the chemosensing ensemble would therefore be advised when only small amounts of interfering electrolytes are present.

Conclusions

We have designed a receptor-based chemosensing ensemble for the fluorimetric detection of chloride in water at near physiological pH. Aqueous chloride is a challenging analyte for this class of sensor since it is extremely well hydrated. Consequently, the literature features only few examples of artificial receptors which are capable of recognizing chloride in neutral aqueous¹⁹ or aqueous/organic media.²⁰ Our sensor can be assembled in situ from easy-to-prepare rhodium(III) receptors (**1** or **2**) and a commercially available fluorescent dye (**3**), and it generates a turn-on signal for sub- to mid-millimolar Cl^- concentrations. The limit of detection is lower than that typically observed for optical chloride sensors based on dynamic quenching.¹ However, like these systems our sensing ensemble also responds to certain heavier halides and pseudo halides (which provoke comparable or greater responses than chloride). It is thus not suited for monitoring chloride in samples which contain substantial quantities of these anions. Of the two receptors we have assessed, the sensor based on cationic **2** is more sensitive while zwitterionic **1** affords greater selectivity; apart from the heavier halides and pseudohalides, only acetate elicits a significant turn-on response in the latter. The signal response and dynamic range for the sensor based on **1** complement those of our previously reported sensing ensemble: indeed, by adding just a small amount of commercially available surfactant, the sensor can be tuned to generate a turn-off signal for low- to mid-micromolar Cl^- concentrations.⁶ Combined, these two sensing ensembles have a dynamic range of more than 3 orders of magnitude (i.e., 5 μM to 30 mM).

Experimental Section

General Information. Trisodium 8-hydroxypyrene-1,3,6-trisulfonate (Sigma-Aldrich), tetrasodium pyrene-1,3,6,8-tetrakisulfonate (Sigma-Aldrich), Ferrozine (Fz) (Acros or Sigma-Aldrich), 2,2'-bipyridine (Sigma-Aldrich), 3-(*N*-morpholino)propanesulfonic acid (MOPS) (Sigma-Aldrich), 2-(*N*-morpholino)ethanesulfonic acid (MES) (Sigma-Aldrich) were purchased and used as received.

(19) For selected examples see: (a) Jiang, X. C.; Yu, A. B. *Langmuir* **2008**, *24*, 4300–4309. (b) Amendola, V.; Bastianello, E.; Fabbrizzi, L.; Mangano, C.; Pallavicini, P.; Perotti, A.; Lanfredi, A. M.; Ugozzoli, F. *Angew. Chem., Int. Ed.* **2000**, *39*, 2917–2920. (c) Goodall, W.; Williams, J. A. G. *J. Chem. Soc., Dalton Trans.* **2000**, 2893–2895. (d) Parker, D.; Senanayake, K.; Williams, J. A. G. *Chem. Commun.* **1997**, 1777. (20) For selected examples see: (a) McConnell, A. J.; Serpell, C. J.; Thompson, A. L.; Allen, D. R.; Beer, P. D. *Chem.—Eur. J.* **2010**, *16*, 1256–1264. (b) Hancock, L. M.; Beer, P. D. *Chem.—Eur. J.* **2009**, *15*, 42–44. (c) Yoon, D.-W.; Gross, D. E.; Lynch, V. M.; Lee, C.-H.; Bennett, P. C.; Sessler, J. L. *Chem. Commun.* **2009**, 1109–1111. (d) Nishiyabu, R.; Palacios, M. A.; Dehaen, W.; Anzenbacher, P., Jr. *J. Am. Chem. Soc.* **2006**, *128*, 11496–11504. (e) Vickers, M. S.; Martindale, K. S.; Beer, P. D. *J. Mater. Chem.* **2005**, *15*, 2784–2790.

(21) (a) Nutton, A.; Bailey, P. M.; Maitlis, P. M. *J. Chem. Soc., Dalton Trans.* **1981**, 1997–2002. (b) Kang, J. W.; Maitlis, P. M. *J. Organomet. Chem.* **1971**, *30*, 127–133.

Complex $[(\text{Cp}^*\text{Rh})_2(\mu\text{-OH})_3](\text{NO}_3)$ was prepared from $[\text{Cp}^*\text{RhCl}(\mu\text{-Cl})_2]$ according to literature procedures.²¹ MOPS buffer solution (pH 7.0) was prepared with bidistilled water. Stock solutions containing appropriate concentrations of all compounds were prepared in MOPS buffer (50 mM, pH 7.0) and stored in the refrigerator.

Physical Measurements. UV/vis spectra were recorded with a Perkin-Elmer Lambda 40 spectrometer using quartz cuvettes with optical path lengths of 0.1, 0.5, or 1.0 cm. Fluorescence spectra were recorded on a Varian Cary Eclipse spectrophotometer equipped with a thermostatted cell holder. ¹H NMR (400 MHz) spectra were recorded on a Bruker Advance DPX 400 spectrometer. Solutions were prepared in 95/5 (v/v) $\text{H}_2\text{O}/\text{D}_2\text{O}$, and spectra were acquired using the zgpgw5 'Watergate' pulse sequence²² for suppression of the water peak. High resolution electrospray ionization mass spectra were obtained with a Waters CapLC-coupled Micro-mass Q-ToF Ultima ESI-instrument.

X-ray Crystallography. Diffraction intensities were measured at 298(2) K for **1** and 100(2) K for $[\text{2}]_2(\text{4}) \cdot 7\text{H}_2\text{O}$ on a STOE IPDSII diffractometer equipped with a graphite monochromated $\text{MoK}\alpha$ radiation source ($\lambda = 0.71073 \text{ \AA}$). Data were reduced using STOE X-Area and corrected for absorption using the integration method.²³ Structure solution, refinement and geometric calculations were performed with SHELX.²⁴ Crystallographic data for **1**: $M = 724.60$, Monoclinic $P2_1/n$, $a = 16.4381(15)$, $b = 11.4858(7)$, $c = 17.6243(14) \text{ \AA}$, $\beta = 117.122(6)^\circ$, $V = 2961.6(4) \text{ \AA}^3$, $Z = 4$; $\rho_{\text{calc}} = 1.625 \text{ Mg m}^{-3}$, $F(000) = 1480$; crystal dimensions $0.10 \times 0.05 \times 0.03 \text{ mm}^3$; $\mu(\text{Mo K}\alpha) = 0.773 \text{ mm}^{-1}$, $T = 298 \text{ K}$. A total of 17903 reflections were measured in the range $2.20 \leq \theta \leq 24.71^\circ$ (hkl range indices: $-19 \leq h \leq 19$, $-13 \leq k \leq 13$, $-20 \leq l \leq 20$), 5043 unique reflections ($R_{\text{int}} = 0.0737$). The structure was refined on F^2 to $R_w = 0.0686$, $R = 0.0470$ (3519 reflections with $I > 2\sigma(I)$) and GOF = 1.018 on F^2 for 490 refined parameters and 233 restraints. Largest peak and hole 0.371 and $-0.500 \text{ e \AA}^{-3}$. CCDC 792102. Crystallographic data for $[\text{2}]_2(\text{4}) \cdot 7\text{H}_2\text{O}$: $M = 1595.33$, Triclinic $P\bar{1}$, $a = 11.1077(11)$, $b = 11.9281(12)$, $c = 13.6309(14) \text{ \AA}$, $\alpha = 77.127(8)$, $\beta = 80.898(8)$, $\gamma = 75.852(8)^\circ$, $V = 1696.9(3) \text{ \AA}^3$, $Z = 1$; $\rho_{\text{calc}} = 1.562 \text{ Mg m}^{-3}$, $F(000) = 826$; crystal dimensions $0.07 \times 0.04 \times 0.02 \text{ mm}^3$; $\mu(\text{Mo K}\alpha) = 0.695 \text{ mm}^{-1}$, $T = 100(2) \text{ K}$. A total of 22193 reflections were measured in the range $2.45 \leq \theta \leq 25.68^\circ$ (hkl range indices: $-13 \leq h \leq 13$, $-14 \leq k \leq 14$, $-16 \leq l \leq 16$), 6454 unique reflections ($R_{\text{int}} = 0.0497$). The structure was refined on F^2 to $R_w = 0.0841$, $R = 0.0455$ (5453 reflections with $I > 2\sigma(I)$) and GOF = 1.086 on F^2 for 478 refined parameters and 27 restraints. Largest peak and hole 0.660 and $-0.806 \text{ e \AA}^{-3}$. CCDC 792103.

Spectrophotometric Titration of Receptor 2 and NaCl. Stock solutions of complex **2** and NaCl in MOPS buffer (50 mM, pH 7.0) were used to prepare a series of solutions with a constant concentration of **2** (500 μM) and a variable concentration of NaCl (0–5 mM). After equilibration at room temperature, the absorption spectra were recorded in the range 300–500 nm (a kinetic study showed that the equilibrium is reached within 1–2 min). The resulting data were fitted to a 1:1 binding isotherm using an in-house built routine in MATLAB which implements evolving factor analysis and a Newton–Gauss multi-non-linear least-squares fitting algorithm.^{25,26} The standard deviations for the fitted parameters ($\log K$) were estimated using the sum-of-squared residuals and inverted curvature matrices as obtained from the iterative fitting processes.

(22) Liu, M.; Mao, X.; He, C.; Huang, H.; Nicholson, J. K.; Lindon, J. C. *J. Magn. Reson.* **1998**, *132*, 125–129.

(23) X-Area, version 1.36; Stoe & Cie, GmbH: Darmstadt, Germany, 2006.

(24) Sheldrick, G. M. *SHELX; Acta Crystallogr., Sect. A* **2008**, *64*, 112–122.

(25) Maeder, M.; Neuhold, Y.-M. In *Practical Data Analysis in Chemistry*; Rutan, S.; Walczak, B., Eds.; Elsevier Publishing Co: Amsterdam, The Netherlands, 2007.

(26) (a) Gamp, H.; Maeder, M.; Meyer, C. J.; Zuberbühler, A. D. *Talanta* **1985**, *23*, 1133–1139. (b) Gamp, H.; Maeder, M.; Meyer, C. J.; Zuberbühler, A. D. *Talanta* **1986**, *33*, 943–951.

Fluorimetric Titrations of 3 with Receptors 1 and 2. Stock solutions of receptor and **3** in MOPS buffer (50 mM, pH 7.0) were used to prepare a series of solutions with a constant **3** concentration (12.5 μM) and a variable concentration of receptor (0–700 μM). The fluorescence emission ($\lambda_{\text{ex}} = 480 \text{ nm}$) at $\lambda_{\text{em}} = 510 \text{ nm}$ were measured after equilibration at room temperature (a kinetic study showed that equilibrium is reached within 2 min). Data fitting was carried out as described above.

Sensing of Chloride. Concentrated solutions of NaCl were added in 1 μL increments to a solution (3 mL) containing receptor (500 μM) and **3** (50 μM) in MOPS buffer (100 mM, pH 7.0). The final Cl^- concentration was 30.0 mM. The fluorescence emission ($\lambda_{\text{ex}} = 480 \text{ nm}$) at $\lambda_{\text{em}} = 510 \text{ nm}$ was measured after each addition following an equilibration period of

5 min at room temperature. Any changes in concentration of receptor and **3** were sufficiently small as to be negligible (<1%). Control experiments with other anions were performed with NaBr, NaF, NaH_2PO_4 , $\text{Na}_4\text{P}_2\text{O}_7$, Na_2SO_4 , NaOAc, NaHCO_3 , NaNO_3 , and sodium salicylate (final conc.: 30.0 mM).

Acknowledgment. We thank Dr. Laure Menin for help with the ESI-MS studies. This work was supported by the Swiss National Science Foundation, by the COST action CM0703 on *Systems Chemistry*, and by the EPFL.

Supporting Information Available: X-ray crystallographic data for **1** and $[\mathbf{2}]_2(\mathbf{4}) \cdot 7\text{H}_2\text{O}$ in CIF format. This material is available free of charge via the Internet at <http://pubs.acs.org>.